

## Article

# Solvent-Free Method for Nanoparticles Synthesis by Solid-State Combustion Using Tetra(Imidazole)Copper(II) Nitrate

Olga V. Netskina <sup>1,\*</sup>, Svetlana A. Mukha <sup>1</sup>, Kirill A. Dmitruk <sup>1</sup>, Arkady V. Ishchenko <sup>1</sup>, Olga A. Bulavchenko <sup>1</sup>, Alena A. Pochtar <sup>1</sup>, Alexey P. Suknev <sup>1</sup> and Oxana V. Komova <sup>1,2</sup>

<sup>1</sup> Boreskov Institute of Catalysis SB RAS, Pr. Akademika Lavrentieva 5, 630090 Novosibirsk, Russia; msa@catalysis.ru (S.A.M.); k.dmitruk@g.nsu.ru (K.A.D.); arcady.ishchenko@gmail.com (A.V.I.); obulavchenko@catalysis.ru (O.A.B.); po4tar@catalysis.ru (A.A.P.); suknev@catalysis.ru (A.P.S.); komova@catalysis.ru (O.V.K.)

<sup>2</sup> Siberian Branch of Russian Academy of Sciences, Pr. Akademika Lavrentieva 17, 630090 Novosibirsk, Russia

\* Correspondence: netskina@catalysis.ru; Tel.: +7-383-330-74-58

**Abstract:** The development of solvent-free techniques for nanoparticles synthesis is one of the challenges of Green chemistry. In this work, the principled opportunity to obtain copper-containing nanosized particles without use of any solvents was shown. The copper complexes were prepared as precursors by the melting-assisted solvent-free synthesis. The formation of tetra(imidazole)copper(II) nitrate complex was confirmed by XRD, elemental analysis, FTIR spectroscopy, and thermal analysis. It was noted that their thermal decomposition occurs in two stages: (I) the low-temperature step may be related to redox interaction between organic ligands and nitrate-anions; (II) the high-temperature step may be related to the oxidation of the products of incomplete imidazole decomposition. TEM and XRD studies of solid products of complex combustion have shown that they are oxides with particle size less than 40 nm. Thus, the combustion of  $[\text{Cu}(\text{Im})_4](\text{NO}_3)_2$  complex under air can be considered as a new approach to prepare nanosized particles of copper oxides without the use of solvents.

**Keywords:** melting-assisted solvent-free synthesis; copper complex; imidazole; nanoparticles



**Citation:** Netskina, O.V.; Mukha, S.A.; Dmitruk, K.A.; Ishchenko, A.V.; Bulavchenko, O.A.; Pochtar, A.A.; Suknev, A.P.; Komova, O.V. Solvent-Free Method for Nanoparticles Synthesis by Solid-State Combustion Using Tetra(Imidazole)Copper(II) Nitrate. *Inorganics* **2022**, *10*, 15. <https://doi.org/10.3390/inorganics10020015>

Received: 20 December 2021

Accepted: 19 January 2022

Published: 21 January 2022

**Publisher's Note:** MDPI stays neutral with regard to jurisdictional claims in published maps and institutional affiliations.



**Copyright:** © 2022 by the authors. Licensee MDPI, Basel, Switzerland. This article is an open access article distributed under the terms and conditions of the Creative Commons Attribution (CC BY) license (<https://creativecommons.org/licenses/by/4.0/>).

## 1. Introduction

The properties of nanomaterials can differ significantly from those of massive objects [1–3]. Qualitatively new characteristics will expand the scope of application of nanoscale materials in mechanical engineering, energetics, optics, electronics, medicine, and chemical industry, including catalytic processes, where the reaction rate depends on the size, morphology, and structure of the catalyst. Composites of different metal-containing phases are especially interesting objects. Their activation can form an active component with a different electronic state of the metal, which essentially affects the rate of chemical transformations [4].

At the moment, various methods for the synthesis of nanomaterials have been proposed, but most of them are expensive and multi-step. Their implementation often requires the auxiliary substances, which must be disposed further, according to the concept of “Green chemistry” [5–7].

One of the solvent-free methods of nanoparticles synthesis is a solid-state combustion (SSC) technique using metal-organic complexes [8,9]. Such complexes should contain energy-intensive ligand and anion-oxidizer, which initiates combustion under short-time heat exposure even in an oxygen-lean environment [10,11]. Due to the rapid redox reactions, the released heat is located in a limited high-temperature zone, where metal-containing nanoparticles are formed. They are well crystallized, so energy-consuming high-temperature calcination is not required.

The synthesis of metal-organic complexes can also be carried out without solvents. The simplest way to synthesize metal-organic complexes is a mixing of starting metal

salts with good chelating ligands in a mortar. This method was successfully implemented to prepare nickel complex with phenanthroline [12] and copper complex simultaneously containing two ligands—4,4-bipyridine and pyrene [13]. To intensify interaction between solid components, reaction mixture undergoes treatment in a ball mill, microwave, or ultrasound reactors [14,15]. For example, the metallamacrocyclic molecular squares were synthesized from (ethylenediamine)Pt(NO<sub>3</sub>)<sub>2</sub> with 4,4'-bipyridyl at room temperature for 10 min of mechanical activation [16]. Note that, in the solution, this process takes up to four weeks at 100 °C [17]. However, mechanochemical activation may be accompanied by local overheating of the reaction mixture, which leads to its phase inhomogeneity and reduces essentially the yield of metal-organic complexes.

More predicted results may be achieved at the synthesis of metal-organic complexes under controlled heating of starting reagents [18]. In this case, highly volatile compounds can interact in the gas phase and then sublime as metal-organic coordination polymer [19]. To prepare metal-organic complexes from thermally stable compounds, melting of their precursors was suggested [8,20]. This approach is easy to implement, and it is also especially interesting for complexes, which should be synthesized in well dried solvents to prevent their complete or partial hydrolysis. In addition, melting-assisted solvent-free synthesis eliminates the labor-consuming step of complexes precipitation in the solution and prolonged drying. Thus, this approach to the synthesis of metal-organic complexes becomes economically attractive.

In our work, tetra(imidazole)copper(II) nitrate was prepared by melting-assisted solvent-free synthesis. Its thermochemical properties and products formed during solid-state combustion have been studied.

## 2. Results and Discussion

### 2.1. Characterization of the Synthesized Copper Complexes

Tetra(imidazole)copper(II) nitrate was prepared by melting-assisted solvent-free synthesis. Its chemical composition was compared with that of complex prepared via precipitation in the solution (Table 1).

**Table 1.** Characterization of the synthesized copper complex.

Complex (Synthesis Method)	Calculated Composition of Complex and Its Molar Mass	Content, wt%		Oxygen Balance, %
		Calculated	Found	
[Cu(C <sub>3</sub> H <sub>4</sub> N <sub>2</sub> ) <sub>4</sub> ](NO <sub>3</sub> ) <sub>2</sub> ( <i>solvent-free</i> )	[Cu(C <sub>3</sub> H <sub>4</sub> N <sub>2</sub> ) <sub>4</sub> ](NO <sub>3</sub> ) <sub>2</sub> or CuC <sub>12</sub> H <sub>16</sub> N <sub>10</sub> O <sub>6</sub> 460 g/mol		Cu–14.2	
			C–30.9	
		Cu–13.9	H–3.4	
		C–31.3	N–30.1	
		H–3.5	Residue–21.4	
	N–30.4			–94
	O–20.9		Cu–13.5	
[Cu(C <sub>3</sub> H <sub>4</sub> N <sub>2</sub> ) <sub>4</sub> ](NO <sub>3</sub> ) <sub>2</sub> ( <i>in aqueous solution</i> )			C–31.4	
			H–3.2	
			N–30.9	
			Residue–21.0	

According to the obtained data (Table 1), copper-containing complexes synthesized in the melt and in aqueous solution have a similar elemental composition, which corresponds to theoretically calculated values for complex compounds with four imidazole molecules as ligands.

The nitrate complexes of copper (II) with imidazole synthesized in the melt of salts with imidazole and in the solution were studied by ATR-FTIR spectroscopy. The obtained results (Figure 1) were correlated with the characteristic frequencies for imidazole and nitrate-anions [21–25].

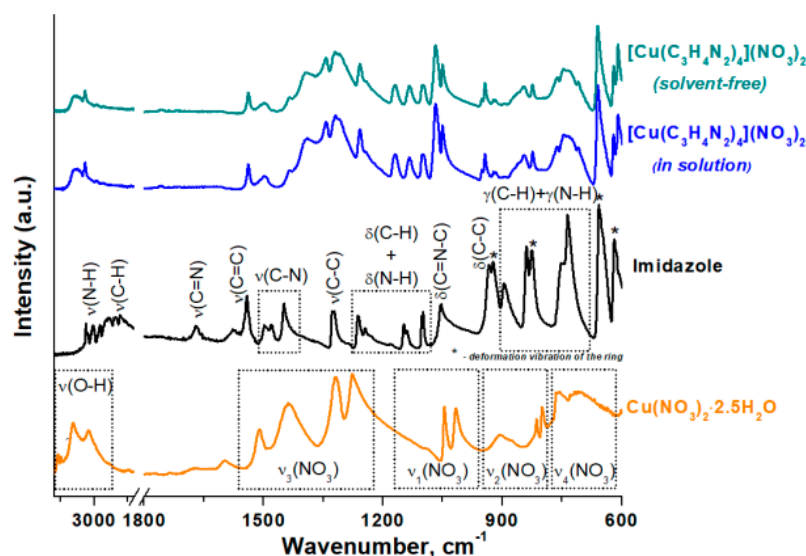


**Figure 1.** FTIR data for nitrate complexes of copper (II) with imidazole synthesized in the melt of copper nitrate with imidazole and in the aqueous solution.

Note that imidazole is a five-membered heterocycle with two nitrogen atoms: (1) weakly acidic group  $>N-H$  and (2) fragment  $-N=$  containing lone pair of electrons which interacts with acidic group  $>N-H$ . In a crystalline state, these groups form hydrogen bonds, which leads to the lower-frequency shift of stretching vibrations of  $N-H$  bond [25], where absorption bands of  $C-H$  stretching vibrations are also observed. In the nitrate complex of copper (II) with imidazole, the higher-frequency shift of  $\nu(N-H)$  bands is observed [26], which indicates the destruction of hydrogen bonds between imidazole molecules due to their direct interaction with metal cations. At the same time, the bands of  $\nu(C=N)$  and  $\nu(C=N-H)$  vibrations shift significantly. Therefore, imidazole coordinates with metal cations due to the lone electron pair of nitrogen, which agrees well with other works [27,28]. The structure of the imidazole ring does not change in the resulting complexes since only a shift of its characteristic bands at  $1700\text{--}600\text{ cm}^{-1}$  is observed. The positive charge of the complex is compensated by nitrate anions. Infrared spectra of the synthesized nitrate complexes of copper (II) with imidazole contain absorption bands at  $700\text{--}760$ ,  $800\text{--}900$ ,  $1050\text{--}1100$ , and  $1300\text{--}1500\text{ cm}^{-1}$  assigned to  $\nu_4(NO_3)$ ,  $\nu_2(NO_3)$ ,  $\nu_1(NO_3)$ , and  $\nu_3(NO_3)$  vibrations [29], respectively.

The nitrate complex of copper (II) with imidazole synthesized in the melt of copper nitrate with imidazole and in the solution were studied by XRD (Figure 2).

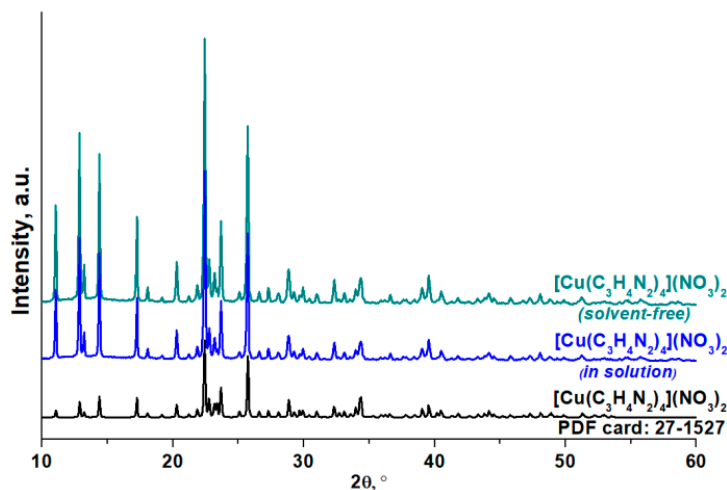


**Figure 2.** XRD pattern of tetra(imidazole)copper(II) nitrate complex prepared by melting-assisted solvent-free synthesis and in the solution.

Comparison of the XRD pattern of the synthesized complex and the simulated one for tetra(imidazole)copper(II) nitrate (PDF card No. 27–1527) confirms the structural identity of these compounds. Thus, it was proved that  $[\text{Cu}(\text{C}_3\text{H}_4\text{N}_2)_4](\text{NO}_3)_2$  was formed as a result of melting-assisted solvent-free synthesis at 90 °C. In addition, the performed studies confirmed the identity of tetra(imidazole)copper(II) nitrate complex synthesized in aqueous solution and via melting of copper nitrate with imidazole.

## 2.2. Thermolysis of Copper Complex Prepared by Melting-Assisted Solvent-Free Synthesis

Thermal analysis was used to study the decomposition of  $[\text{Cu}(\text{C}_3\text{H}_4\text{N}_2)_4](\text{NO}_3)_2$  complex prepared by melting-assisted solvent-free synthesis. The experiments were performed in inert (helium) and oxidizing (air) environment at a heating rate of 5 °C/min. The obtained data are shown in Figure 3, where the comparison of TG and DSC curves of synthesized complex and imidazole is carried out.

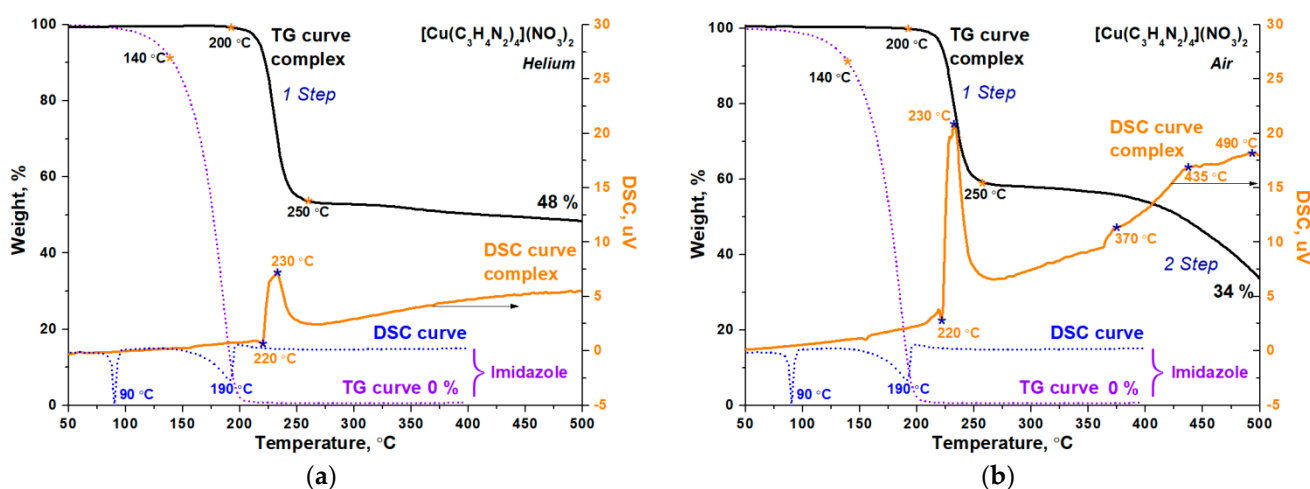


**Figure 3.** Thermal analysis data for  $[\text{Cu}(\text{C}_3\text{H}_4\text{N}_2)_4](\text{NO}_3)_2$  complex prepared by melting-assisted solvent-free synthesis. Heating rate is 5 °C/min in (a) helium and (b) air.

It was found that the DSC curve of imidazole is characterized by endothermic effects due to its melting and evaporation. The temperature of these phase transitions does not depend on the gas composition, where the heating occurs (Figure 3). The first phase transition “solid-liquid” is observed at 90 °C and is not accompanied by the weight loss. The phase transition “liquid-gas” starts at 140 °C and completes at 190 °C with total weight loss due to the evaporation. For a copper complex, these endothermic effects are not observed, indicating the absence of free imidazole impurities in the sample prepared by melting-assisted solvent-free synthesis.

The decomposition of  $[\text{Cu}(\text{C}_3\text{H}_4\text{N}_2)_4](\text{NO}_3)_2$  complex starts at 200 °C. One step of sharp change of the sample weight in helium and two steps in air can be clearly distinguished on TG curves, which are accompanied by exothermic effects. The temperature of the first step does not depend on the gas composition since it is assumed [30] that oxidation of organic ligands by nitrate-anions occurs in this temperature range. Analyzing the thermolysis data of  $[\text{Cu}(\text{C}_3\text{H}_4\text{N}_2)_4](\text{NO}_3)_2$  complex at heating of 5 °C/min in helium and air, the kinetic parameters of this process were estimated according to Equation [31]:

$$\frac{d\alpha}{dT} = \frac{A}{\beta} e^{-\frac{E}{RT}} (1 - \alpha)^n, \quad (1)$$

where  $\frac{d\alpha}{dt}$ —reaction rate, expressed as the change in the degree of conversion ( $\alpha$ ) per unit time ( $t$ ),  $A$ —pre-exponential factor,  $\beta$ —linear heating rate (constant),  $E$ —activation

energy,  $R$ —gas constant,  $T$ —temperature, and  $n$ —order of reaction. The linearization of this equation performed by the method of Coats and Redfern [32]:

$$\ln\left\{\frac{-\ln(1-\alpha)}{T^2}\right\} = \ln\frac{AR}{\beta E}\left(1 - \frac{2RT}{E}\right) - \frac{E}{RT} \quad (2)$$

The obtained kinetic parameters for the first step of  $[\text{Cu}(\text{C}_3\text{H}_4\text{N}_2)_4](\text{NO}_3)_2$  complex decomposition are summarized in Table 2.

**Table 2.** The kinetic parameters of the first step of thermal decomposition for tetra(imidazole)copper(II) nitrate prepared by melting-assisted solvent-free synthesis.

Method	Parameter	Helium	Air
Coats-Redfern	E, kJ/mol	246	236
	n	1	1
	$\alpha$ <sup>1</sup>	0.01–0.80	0.01–0.60
	R <sup>2</sup>	0.994	0.990

<sup>1</sup>—sample conversion range calculated basing on current weights related to the beginning and the end of analyzed TG ranges, and sample weight at the end of thermal analysis at 500 °C.

As follows from the comparison of maximal values of the correlation coefficient ( $R^2$ ), the best description of the experimental data is achieved using the first-order kinetic model of Coats–Redfern, which are characteristic of monomolecular decomposition reactions [33]. Based on the performed calculations, the activation energies for decomposition of the complex in oxidizing and inert medium were determined. It should be noted that the activation energy is lower in the presence of oxygen than in helium. However, the difference is only 10 kJ/mol, which indicates a similar character of the ligand interaction with nitrate-anion in inert and oxygen-containing environments.

At a temperature below 250 °C, complete decomposition of the studied metal-organic compounds does not occur, since tetra(imidazole)copper(II) nitrate has a highly negative oxygen balance (Table 1). Hence, further heating leads to a decrease in the sample weight. In the presence of oxygen, the products of incomplete imidazole decomposition are oxidized with a noticeable heat release, which is reflected in the TG curve (Figure 3b). The  $[\text{Cu}(\text{C}_3\text{H}_4\text{N}_2)_4](\text{NO}_3)_2$  complex is characterized by slow oxidation of the products of incomplete imidazole decomposition with weakly pronounced exothermic effects at 370, 435, and 490 °C in the studied temperature range.

### 2.3. Solid Products of Combustion of Copper Complex Prepared by Melting-Assisted Solvent-Free Synthesis

Combustion of tetra(imidazole)copper(II) nitrate was carried out by heating its powder in a corundum crucible under air. When a certain temperature was reached, spontaneous ignition occurred with the formation of solid products, which were studied in detail. According to TEM data, the solid products of  $[\text{Cu}(\text{C}_3\text{H}_4\text{N}_2)_4](\text{NO}_3)_2$  combustion are large aggregates of different morphology (Figure 4a) consisting of smaller particles (Figure 4b). Local analysis of the crystal structure of individual particles (Figure 4c and d) showed that they are copper oxides  $\text{Cu}_2\text{O}$  (PDF No. 5–667: [220]–1.5100 Å) or  $\text{CuO}$  (PDF No. 45–937: [–113]–1.5058 Å; [22]–1.4184 Å; [112]–1.7769 Å). Metal particles were also detected (PDF No. 4–836: [220]–1.2780 Å; [311]–1.0900 Å). They are surrounded by the shell of amorphous carbon (Figure 4d), which seems to prevent their oxidation during combustion.

The XRD analysis (Figure 5) also confirmed preferential formation of the oxides (Table 3) during combustion of the  $[\text{Cu}(\text{C}_3\text{H}_4\text{N}_2)_4](\text{NO}_3)_2$  complex prepared by melting-assisted solvent-free synthesis. An impurity of the reduced metal (~2 wt%) was found. The crystallite size of the formed phases lies within the nanoscale, being less than 40 nm for the oxides. Larger crystallites are characteristic of metallic copper, but their size does not exceed 80 nm.

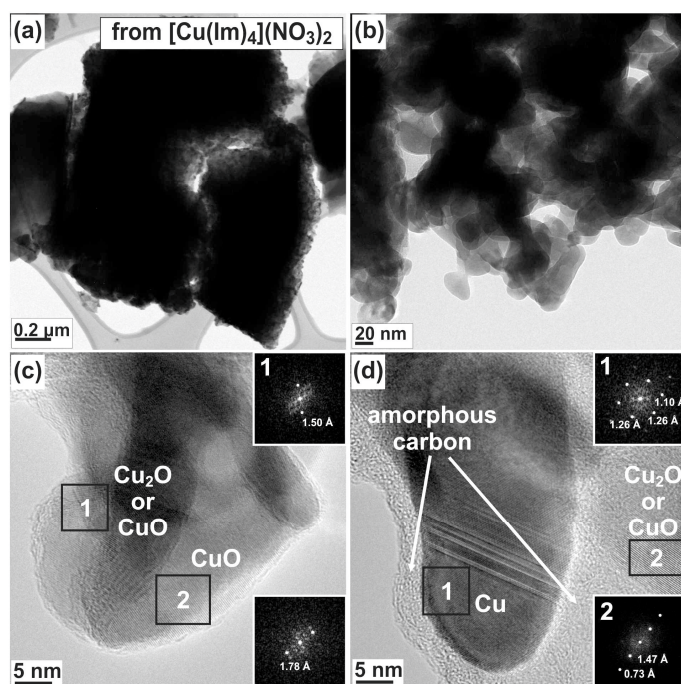


**Figure 4.** TEM data for solid products obtained by combustion of  $[\text{Cu}(\text{C}_3\text{H}_4\text{N}_2)_4](\text{NO}_3)_2$  complex under air: (a,b) morphology and (c,d) fast Fourier transform (FFT) patterns are calculated from the TEM image of individual particles.

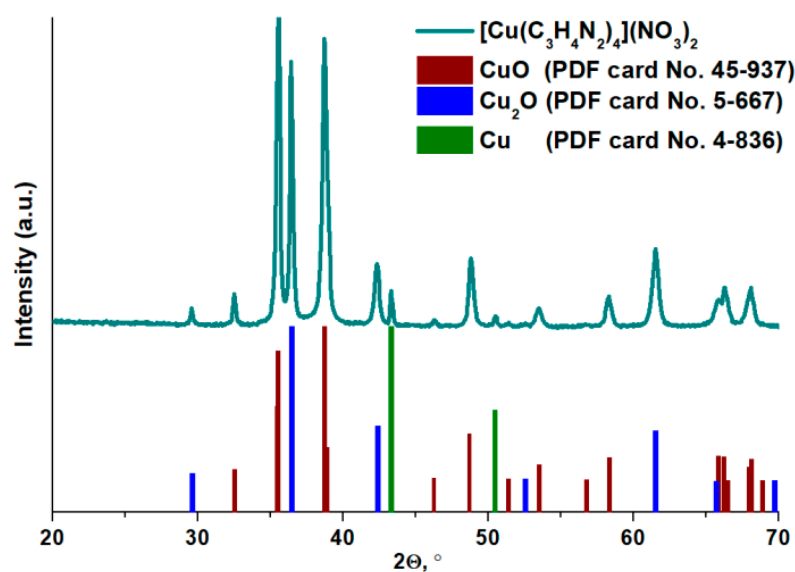


**Figure 5.** XRD data for solid products obtained by combustion of  $[\text{Cu}(\text{C}_3\text{H}_4\text{N}_2)_4](\text{NO}_3)_2$  complex under air.

**Table 3.** XRD data for solid products obtained by combustion of  $[\text{Cu}(\text{C}_3\text{H}_4\text{N}_2)_4](\text{NO}_3)_2$  complex under air.

Complex	Phase	No. PDF Card	Content, wt%	Average Crystallite Size, nm	
				LVol-IB	LVol-FWHM
$[\text{Cu}(\text{C}_3\text{H}_4\text{N}_2)_4](\text{NO}_3)_2$	CuO	45-937	74	28	37
	$\text{Cu}_2\text{O}$	5-667	24	30	37
	Cu	4-836	2	76	72

Thus, the combustion of  $[\text{Cu}(\text{C}_3\text{H}_4\text{N}_2)_4](\text{NO}_3)_2$  complex under air can be considered as a new approach to prepare copper oxides with nanosized particles without the use of solvents. Herewith, it is possible to change the ratio between copper-containing phases in the sample by varying the combustion conditions, as was shown for glycine-nitrate compositions of copper and nickel [30,34].

### 3. Materials and Methods

#### 3.1. Materials

Commercial reagents were used for the synthesis of complexes: copper (II) nitrate  $\text{Cu}(\text{NO}_3)_2 \cdot 2.5\text{H}_2\text{O}$  (Sigma-Aldrich, St. Louis, MO, USA, CAS 19004-19-4, 98%), imidazole  $\text{C}_3\text{H}_4\text{N}_2$  (Sigma-Aldrich, St. Louis, MO, USA, CAS 288-32-4, 99%), ethanol  $\text{C}_2\text{H}_5\text{OH}$  (Sigma-Aldrich, St. Louis, MO, USA, CAS 64-17-5, 95%).

#### 3.2. Synthesis of Copper Complex

$[\text{Cu}(\text{C}_3\text{H}_4\text{N}_2)_4](\text{NO}_3)_2$  (*melting-assisted solvent-free synthesis*) The synthesis was performed within a ceramic crucible at 90 °C. When copper (II) nitrate (0.01 mol) was added in a colorless imidazole (0.04 mol), a reaction mixture was colored in purple, and then crystallized instantly as a powder. The sample was stored in a desiccator over  $\text{P}_2\text{O}_5$ . The product yield was 97%.

$[\text{Cu}(\text{C}_3\text{H}_4\text{N}_2)_4](\text{NO}_3)_2$  (*in solution*) At room temperature, copper nitrate (0.01 mol) was added to an aqueous solution of imidazole (0.04 mol). Within 5 min of stirring, a purple precipitate formed. It was filtered, washed by cold water and ethanol. Then, it was dried and stored in a desiccator over  $\text{P}_2\text{O}_5$ . The product yield was 65 %.

Using the following equation, the oxygen balance was determined:

$$\text{Oxygen balance (\%)} = \frac{-1600}{\text{Molar mass}} \cdot (2\text{C} + \frac{\text{H}}{2} + \text{M} - \text{O}), \quad (3)$$

where C—quantity of carbon atoms, H—quantity of hydrogen atoms, O—quantity of oxygen atoms, and M—quantity of metal atoms. The oxygen balance is the ratio between the amount of oxygen in a chemical and the amount of oxygen needed to ensure the complete oxidation of all the components of chemical.

#### 3.3. Combustion of Copper Complex

Combustion procedure of complex was performed under air. A corundum crucible with complex powder was placed on the heated surface of an IKA-C-Mag HS4 tile (IKA, Königswinter, Germany) at a predetermined temperature of 500 °C. During a few minutes, a rapid heating of the sample occurred, followed by spontaneous ignition. The solid products of complex combustion were loose powders that were stored in a desiccator over  $\text{P}_2\text{O}_5$ .

#### 3.4. Characterization of Complex and Solid Products of Combustion

The Cu content was defined by inductively coupled plasma atomic emission spectrometry on an Optima 4300 DV (PerkinElmer, Waltham, MA, USA). Using an automatic CHNS analyzer EURO EA 3000 (Euro Vector S.p.A., Castellanza, Italy), the carbon, hydrogen, and nitrogen contents were determined. In the dynamic regime (a vertical reactor) at 1050 °C in a flow of He with added oxygen, the complexes (0.5–2 mg) were combusted. The measurement error is in the range of  $\pm 3\%$ . In Table 1, the obtained data were given.

IR spectra were obtained by the attenuated total reflection infrared spectroscopy (ATR FTIR) using an Agilent Cary 600 spectrometer (Agilent Technologies, Santa Clara, CA, USA) equipped with a Gladi ATR attachment (PIKE Technologies, Madison, WI, USA).

The thermolysis of synthesized complexes was studied on a Netzsch STA 449 C Jupiter instrument equipped with a DSC/TG holder (NETZSCH, Selb, Germany) in the temperature range of 30–500 °C under a flow of helium and air ( $30 \text{ mL} \cdot \text{min}^{-1}$ ). The heating rate was  $5 \text{ }^\circ\text{C} \cdot \text{min}^{-1}$ . The sample weight was 5 mg.

By a ThemisZ electron microscope (Thermo Fisher Scientific, Waltham, MA, USA) with an accelerating voltage of 200 kV and a limiting resolution of 0.07 nm, the samples were studied. Samples for research were fixed on standard aluminum grids using ultrasonic dispersion in ethanol.

The synthesized complex and solid products of combustion were characterized by a powder XRD technique using a D8 Advance diffractometer equipped with a Lynxeye linear detector (Bruker AXS GmbH, Karlsruhe, Germany). The XRD patterns were obtained in the  $2\theta$  range from 15 to  $80^\circ$  with a step of  $0.05^\circ$  (accumulation time—3 s).  $\text{CuK}\alpha$  radiation ( $\lambda = 1.5418 \text{ \AA}$ ) was used. The composition of the gasification products was identified by the Rietveld method [35] using the TOPAS program (TOPAS—Total Pattern Analysis System, Version 4.2, Bruker AXS GmbH, Karlsruhe, Germany). The instrumental broadening was described with metallic silicon as reference material. The size of the coherent scattering domain was calculated using LVol-IB values (LVol-IB—the volume-weighted mean column height based on integral breadth) and LVol-FWHM (the volume-weighted mean column height based on full width at half maximum,  $k = 0.89$ ).

#### 4. Conclusions

The work demonstrates the possibility of solvent-free synthesis of tetra(imidazole)copper(II) nitrate complex via imidazole melting with copper nitrate. It was found that their elemental composition corresponds to theoretically calculated values for complex compounds with four imidazole molecules as ligands. FTIR spectroscopy and thermal analysis data confirm the incorporation of imidazole into the immediate environment of the metal cation. Comparison of XRD pattern of the synthesized complex and the simulated one for tetra(imidazole)copper(II) nitrate confirmed the structural identity of these compounds. Thus, it was proved that melting-assisted solvent-free synthesis at  $90^\circ\text{C}$  resulted in  $[\text{Cu}(\text{C}_3\text{H}_4\text{N}_2)_4](\text{NO}_3)_2$  formation.

It was noted that the decomposition of  $[\text{Cu}(\text{C}_3\text{H}_4\text{N}_2)_4](\text{NO}_3)_2$  complex has a stepwise character of weight loss. The first weight loss corresponds to redox interreaction of organic ligand with nitrate-anions, and its temperature is the same in both inert and oxidizing atmosphere. Herewith, the calculated activation energies were 246 and 236 kJ/mol, respectively. Such close values confirm the identity of the ligand interaction with nitrate-anions in helium and air flows. The second weight loss is observed only in the presence of oxygen and is caused by the oxidation of the products of incomplete imidazole decomposition.

Tetra(imidazole)copper(II) nitrate was used to obtain copper-containing nanoparticles by solid-state combustion. Copper oxides ( $\text{Cu}_2\text{O}$  and  $\text{CuO}$ ) with a small impurity of the reduced metal are identified as combustion products, which can be used as effective catalysts for methanol oxidation carbonylation [36], conversion of nitrophenol to aminophenol [37], photocatalytic hydrogen evolution [38], etc. Therefore, the combustion of  $[\text{Cu}(\text{C}_3\text{H}_4\text{N}_2)_4](\text{NO}_3)_2$  complex under air can be considered as a new approach to prepare copper oxides with nanosized particles without the use of solvents. It is shown in work [39–41] that, by varying the combustion conditions, it is possible to purposefully prepare oxides and metals in a highly dispersed state. This direction is very promising and will be further developed by us for the synthesis of catalysts, which do not require a high-temperature step of their activation in hydrogen to form a catalytically active phase [8].

**Author Contributions:** Conceptualization, O.V.N. and O.V.K.; methodology, S.A.M. and K.A.D.; formal analysis, A.P.S. and K.A.D.; investigation, O.V.N., A.V.I., and O.A.B.; data curation, A.P.S., O.A.B., A.A.P., and A.V.I.; writing—original draft preparation, S.A.M. and A.A.P.; writing—review and editing, O.V.N.; supervision, O.V.K.; project administration, O.V.N. All authors have read and agreed to the published version of the manuscript.

**Funding:** This research was funded by the Ministry of Science and Higher Education of the Russian Federation (project No. 075-15-2020-781).

**Institutional Review Board Statement:** Not applicable.

**Informed Consent Statement:** Not applicable.

**Data Availability Statement:** Not applicable.

**Conflicts of Interest:** The authors declare no conflict of interest.

## References

1. Donegá, C.d.M. *Nanoparticles: Workhorses of Nanoscience*, 1st ed.; Springer: Berlin/Heidelberg, Germany, 2014; p. 299.
2. Buffat, P.; Borel, J.-P. Size effect on the melting temperature of gold particles. *Phys. Rev. A* **1976**, *13*, 2287–2298. [[CrossRef](#)]
3. Wang, Z.L.; Petroski, J.M.; Green, T.C.; El-Sayed, M.A. Shape transformation and surface melting of cubic and tetrahedral platinum nanocrystals. *J. Phys. Chem. B* **1998**, *102*, 6145–6151. [[CrossRef](#)]
4. Netskina, O.V.; Kochubey, D.I.; Prosvirin, I.P.; Kellerman, D.G.; Simagina, V.I.; Komova, O.V. Role of the electronic state of rhodium in sodium borohydride hydrolysis. *J. Mol. Catal. A* **2014**, *390*, 125–132. [[CrossRef](#)]
5. Hos, T.; Herskowitz, M. Utilization of CO-rich waste gases from the steel industry for production of renewable liquid fuels. *Energ. Convers. Manag.* **2021**, *240*, 114233. [[CrossRef](#)]
6. Netskina, O.V.; Tayban, E.S.; Moiseenko, A.P.; Komova, O.V.; Mukha, S.A.; Simagina, V.I. Removal of 1,2-dichlorobenzene from water emulsion using adsorbent catalysts and its regeneration. *J. Hazard. Mater.* **2015**, *285*, 84–93. [[CrossRef](#)] [[PubMed](#)]
7. Tkachenko, I.; Tkachenko, S.N.; Lokteva, E.S.; Mamleeva, N.A.; Lunin, V.V. Two-stage ozonation–adsorption purification of ground water from trichloroethylene and tetrachloroethylene with application of commercial carbon adsorbents. *Ozone Sci. Eng.* **2020**, *42*, 357–370. [[CrossRef](#)]
8. Netskina, O.V.; Mucha, S.S.; Veselovskaya, J.V.; Bolotov, V.A.; Komova, O.V.; Ishchenko, A.V.; Bulavchenko, O.A.; Prosvirin, I.P.; Pochtar, A.A.; Rogov, V.A. CO<sub>2</sub> methanation: Nickel-alumina catalyst prepared by solid-state combustion. *Materials* **2021**, *14*, 6789. [[CrossRef](#)]
9. Komova, O.V.; Mukha, S.A.; Ozerova, A.M.; Bulavchenko, O.A.; Pochtar, A.A.; Ishchenko, A.V.; Odegova, G.V.; Suknev, A.P.; Netskina, O.V. New solvent-free melting-assisted preparation of energetic compound of nickel with imidazole for combustion synthesis of ni-based materials. *Nanomaterials* **2021**, *11*, 3332. [[CrossRef](#)]
10. Tappan, B.C.; Huynh, M.H.; Hiskey, M.A.; Chavez, D.E.; Luther, E.P.; Mang, J.T.; Son, S.F. Ultralow-density nanostructured metal foams: Combustion synthesis, morphology, and composition. *J. Am. Chem. Soc.* **2006**, *128*, 6589–6594. [[CrossRef](#)]
11. Boldyrev, V.V.; Tukhtaev, R.K.; Gavrilov, A.I.; Larionov, S.V.; Savel'eva, Z.A.; Lavrenova, L.G. Combustion of nickel and copper nitrate complexes of hydrazine derivatives as a method for manufacturing fine-grained and porous metals. *Russ. J. Inorg. Chem.* **1998**, *43*, 362–366.
12. Nichols, P.J.; Raston, C.L.; Steed, J.W. Engineering of porous  $\pi$ -stacked solids using mechanochemistry. *Chem. Commun.* **2001**, *12*, 1062–1063. [[CrossRef](#)]
13. Tella, A.C.; Ameen, O.A.; Ajibade, P.A.; Alimi, L.O. Template metal-organic frameworks: Solvent-free synthesis, characterization and powder X-ray diffraction studies of [Cu(NO<sub>3</sub>)<sub>2</sub>(bipy)<sub>2</sub>](py)<sub>2</sub>. *J. Porous Mater.* **2015**, *22*, 1599–1605. [[CrossRef](#)]
14. Zangade, S.; Patil, P. A Review on solvent-free methods in organic synthesis. *Curr. Org. Chem.* **2019**, *23*, 2295–2318. [[CrossRef](#)]
15. Fernández-Bertran, J.F. Mechanochemistry: An overview. *Pure Appl. Chem.* **1999**, *71*, 581–586. [[CrossRef](#)]
16. Orita, A.; Jiang, L.; Nakano, T.; Ma, N.; Otera, J. Solventless reaction dramatically accelerates supramolecular self-assembly. *Chem. Commun.* **2002**, *13*, 1362–1363. [[CrossRef](#)]
17. Fujita, M.; Yazaki, J.; Ogura, K. Spectroscopic observation of self-assembly of a macrocyclic tetranuclear complex composed of Pt<sup>2+</sup> and 4,4'-bipyridine. *Chem. Lett.* **1991**, *20*, 1031–1032. [[CrossRef](#)]
18. Garay, A.L.; Pichona, A.; James, S.L. Solvent-free synthesis of metal complexes. *Chem. Soc. Rev.* **2007**, *36*, 846–855. [[CrossRef](#)] [[PubMed](#)]
19. Filatov, A.S.; Rogachev, A.Y.; Petrukhina, M.A. Gas-phase assembling of dirhodium units into a novel organometallic ladder: structural and DFT study. *Cryst. Growth Des.* **2006**, *6*, 1479–1484. [[CrossRef](#)]
20. Taylor, C.E.; Underhill, A.E. Complexes of cobalt(II) and nickel(II) halides with Imidazole. *J. Chem. Soc. A* **1969**, 368–372. [[CrossRef](#)]
21. Trivedi, M.K.; Branton, A.; Trivedi, D.; Nayak, G.; Saikia, G.; Jana, S. Physical and structural characterization of biofield treated imidazole derivatives. *Nat. Prod. Chem. Res.* **2015**, *3*, 1000187. [[CrossRef](#)]
22. Madanagopal, A.; Periandy, S.; Gayathri, P.; Ramalingam, S.; Xavier, S.; Ivanov, V.K. Spectroscopic and computational investigation of the structure and pharmacological activity of 1-benzylimidazole. *J. Taibah Univ. Sci.* **2017**, *11*, 975–996. [[CrossRef](#)]
23. Van Bael, M.K.; Smets, J.; Schoone, K.; Houben, L.; McCarthy, W.; Adamowicz, L.; Nowak, M.J.; Maes, G. Matrix-isolation FTIR studies and theoretical calculations of hydrogen-bonded complexes of imidazole. A Comparison between Experimental Results and Different Calculation Methods. *J. Phys. Chem. A* **1997**, *101*, 2397–2413. [[CrossRef](#)]
24. Ramasamy, R. Vibrational spectroscopic studies of imidazole. *Armen. J. Phys.* **2015**, *8*, 51–55.
25. Morzyk-Ociepa, B.; Różycka-Sokołowska, E.; Michalska, D. Revised crystal and molecular structure, FT-IR spectra and DFT studies of chlorotetrakis(imidazole)copper(II) chloride. *J. Mol. Struct.* **2012**, *1028*, 49–56. [[CrossRef](#)]
26. Lee, S.-K.; Lee, S.-J.; Ahn, A.-R.; Kim, Y.-S.; Min, A.-R.; Choi, M.-Y.; Miller, R. E. Infrared Spectroscopy of Imidazole Trimer in Helium Nanodroplets: Free NH Stretch Mode. *Bull. Korean Chem. Soc.* **2011**, *32*, 885–888. [[CrossRef](#)]
27. Eilbeck, W.J.; Holmes, F.; Underhill, A.E. Cobalt(II), nickel(II), and copper(II) complexes of imidazole and thiazole. *J. Chem. Soc. A* **1967**, 757–761. [[CrossRef](#)]

28. Amini, S.K.; Hadipour, N.L.; Elmi, F. A study of hydrogen bond of imidazole and its 4-nitro derivative by ab initio and DFT calculated NQR parameters. *Chem. Phys. Lett.* **2004**, *391*, 95–100. [[CrossRef](#)]
29. Mihaylov, M.Y.; Zdravkova, V.R.; Ivanova, E.Z.; Aleksandrov, H.A.; Petkov, P.S.; Vayssilov, G.N.; Hadjiivanov, K.I. Infrared spectra of surface nitrates: Revision of the current opinions based on the case study of ceria. *J. Catal.* **2021**, *394*, 245–258. [[CrossRef](#)]
30. Kumar, A.; Wolf, E.E.; Mukasyan, A.S. Solution combustion synthesis of metal nanopowders: Copper and copper/nickel alloys. *AIChE J.* **2011**, *57*, 3473–3479. [[CrossRef](#)]
31. Zsako, J. Kinetic analysis of thermogravimetric data. *J. Phys. Chem.* **1968**, *72*, 2406–2411. [[CrossRef](#)]
32. Coats, A.W.; Redfern, J.P. Kinetic parameters from thermogravimetric data. *Nature* **1964**, *201*, 68–69. [[CrossRef](#)]
33. Fetisova, O.Y.; Mikova, N.M.; Chesnokov, N.V. A kinetic study of the thermal degradation of fir and aspen ethanol lignins. *Kinet. Catal.* **2019**, *60*, 273–280. [[CrossRef](#)]
34. Kumar, A.; Wolf, E.E.; Mukasyan, A.S. Solution combustion synthesis of metal nanopowders: Nickel—Reaction pathways. *AIChE J.* **2011**, *57*, 2207–2214. [[CrossRef](#)]
35. Rietveld, H.M. A profile refinement method for nuclear and magnetic structures. *J. Appl. Crystallogr.* **1969**, *2*, 65–71. [[CrossRef](#)]
36. Wang, J.; Fu, T.; Meng, F.; Zhao, D.; Chuang, S.S.C.; Li, Z. Highly active catalysis of methanol oxidative carbonylation over nano Cu<sub>2</sub>O supported on micropore-rich mesoporous carbon. *Appl. Catal. B* **2022**, *303*, 120890. [[CrossRef](#)]
37. Verma, A.; Anand, P.; Kumar, S.; Fu, Y.-P. Cu-cuprous/cupric oxide nanoparticles towards dual application for nitrophenol conversion and electrochemical hydrogen evolution. *Appl. Surf. Sci.* **2022**, *578*, 151795. [[CrossRef](#)]
38. Hu, S.; Shi, J.; Luo, B.; Ai, C.; Jing, D. Significantly enhanced photothermal catalytic hydrogen evolution over Cu<sub>2</sub>O-rGO/TiO<sub>2</sub> composite with full spectrum solar light. *J. Colloid Interface Sci.* **2022**, *608*, 2058–2065. [[CrossRef](#)]
39. Manukyan, K.V.; Cross, A.; Roslyakov, S.; Rouvimov, S.; Rogachev, A.S.; Wolf, E.E.; Mukasyan, A.S. Solution Combustion Synthesis of Nano-Crystalline Metallic Materials: Mechanistic Studies. *J. Phys. Chem. C* **2013**, *117*, 24417–24427. [[CrossRef](#)]
40. Podbolotov, K.B.; Khort, A.A.; Tarasov, A.B.; Trusov, G.V.; Roslyakov, S.I.; Mukasyan, A.S. Solution Combustion Synthesis of Copper Nanopowders: The Fuel Effect. *Combust. Sci. Technol.* **2017**, *189*, 1878–1890. [[CrossRef](#)]
41. Sheng, N.; Zhu, C.; Rao, Z. Solution combustion synthesized copper foams for enhancing the thermal transfer properties of phase change material. *J. Alloys Compd.* **2021**, *871*, 159458. [[CrossRef](#)]